Pergamon

Biochemical Pharmacology, Vol. 47, No. 2, pp. 317–329, 1994.

0006-2952/94 $6.00 + 0.00

0006-2952(93)E0005-R

INFLUENCE OF AMSACRINE (m-AMSA) ON BULK AND GENE-SPECIFIC DNA DAMAGE AND c-*myc* EXPRESSION IN MCF-7 BREAST TUMOR CELLS

RODERICK T. BUNCH,*† LAWRENCE F. POVIRK,* MICHAEL S. ORR,* JOYCE K. RANDOLPH,‡ FRANK A. FORNARI* and DAVID A. GEWIRTZ*‡§

Departments of *Pharmacology and Toxicology, and ‡Medicine, Virginia Commonwealth University/Medical College of Virginia, Richmond, VA 23298, U.S.A.

(*Received* 1 *June* 1993; *accepted* 31 *August* 1993)

Abstract—In the MCF-7 human breast tumor cell line, the aminoacridine, m-AMSA, induces protein-associated DNA strand breaks consistent with inhibition of topoisomerase II. However, neither single-strand nor double-strand breaks in DNA, determined using conventional assays, show a consistent relationship with m-AMSA-induced inhibition of growth. In contrast, when DNA strand breaks are determined by alkaline unwinding under the high salt conditions of the alkaline unwinding/Southern blotting (AU/SB) assay, developed by our laboratories, damage to DNA corresponds closely with growth inhibition. The AU/SB assay, which is capable of assessing breaks within large-scale domains (upwards of 1 megabase) surrounding genes of interest, was further utilized to explore the capacity of m-AMSA to induce damage within specific genomic regions that may regulate cell growth. Regions *encompassing* the transcriptionally active oncogenes, c-*myc* and c-*fos*, were found to be more susceptible to m-AMSA-induced strand breaks than the region encompassing the non-transcribed α-satellite DNA or the genome as a whole (bulk DNA). These findings demonstrate that m-AMSA may produce more pronounced damage within specific genomic regions than in bulk DNA. m-AMSA also preferentially altered expression of the c-*myc* oncogene; at an m-AMSA concentration where growth was inhibited by between 70 and 80%, steady-state c-*myc* mRNA levels declined to approximately 10–15% of control levels within 2–3 hr; furthermore, concentration-dependent reductions in c-*myc* expression appeared to coincide with growth inhibition. In addition, inhibition of [^{3}H]thymidine incorporation after 2 hr directly paralleled inhibition of growth, suggesting an early effect at the level of DNA biosynthesis, possibly related to the down-regulation of c-*myc* expression. It is proposed that specific lesions, e.g., in regions surrounding the c-*myc* gene, as well as generalized lesions in DNA may lead to growth inhibition mediated by down-regulation of the expression of select growth regulatory genes, such as c-*myc*.

Key words: c-*myc*, m-AMSA, DNA damage

Various classes of antineoplastic drugs, including the anthracycline antibiotics, the epipodophyllotoxins, and the aminoacridines have been shown to interfere with the religation activity of DNA topoisomerase II via stabilization of the DNA–topoisomerase II "cleavable complex" [1–4]. Stabilization of the cleavable complex and the concomitant induction of bulk DNA damage (i.e. DNA strand breaks) have been shown to correspond closely with drug toxicity and/or antiproliferative activity [5], suggesting that these bulk DNA lesions mediate the antitumor effects of topoisomerase II inhibitors. In contrast, recent evidence from our laboratories [6] and work by other investigators [7, 8] suggest that bulk or overall DNA strand breakage may not always correlate with the antineoplastic activity of topoisomerase II inhibitors.

It has been hypothesized that the antineoplastic activity of the topoisomerase II inhibitors may be the result of a specific subset of bulk DNA lesions, which occur in chromatin regions critical for the viability and growth of the neoplastic cell [7]. Studies by Riou *et al.* [9, 10] have demonstrated that the aminoacridine, m-AMSA,‖ a topoisomerase II inhibitor, induces breaks within the c-*myc* gene and alters c-*myc* expression. More recently, it has been shown that m-AMSA induces strong topoisomerase II-mediated cleavage sites within the c-*myc* promoter region [11]. These findings suggest that the c-*myc* locus may be uniquely susceptible to DNA damage. Damage in regions surrounding the c-*myc* gene may have important consequences for cytotoxicity as the MYC protein is associated with the nuclear matrix, particularly during S phase [12], and has been shown to be an important regulator of growth in human breast tumor cell lines [13–15].

† Present address: Dept. of Pharmacology, Dartmouth Medical School, Hanover, NH 03155.

§ Corresponding author: Dr. David A. Gewirtz, Department of Medicine, Virginia Commonwealth University/Medical College of Virginia, Box 230 MCV Station, Richmond, VA 23298. Tel. (804) 786-9523; FAX (804) 371-8079.

‖ Abbreviations: m-AMSA, amsacrine, 4′-(9-acridinylamino)methanesulfon-*m*-anisidide; SDS, sodium dodecyl sulfate; TCA, trichloroacetic acid; ssDNA, single-stranded DNA; SSB, single-strand break; DSB, double-strand break; %dsDNA, per cent of total DNA remaining double stranded (acid-precipitable DNA/total DNA × 100); F_{DS}, fraction of hybridization sequence remaining double-stranded compared with control (density of hybridization signal treated sample/control); GAPD, glyceraldehyde phosphate dehydrogenase; and AU/SB, alkaline unwinding/Southern blot.

Studies in our own laboratories assessing damage to specific genomic regions in MCF-7 breast tumor cells exposed to the demethylepipodophyllotoxin derivative VM-26 (teniposide) support the susceptibility of the c-*myc* region to damage induced by topoisomerase II inhibitors [16]. The present studies were designed to examine the influence of m-AMSA on bulk and region-specific damage and on c-*myc* expression in the MCF-7 breast tumor cell line in order to explore the potential consequences of such perturbations on cell growth.

MATERIALS AND METHODS

Materials. Dulbecco's Modified Eagle's Medium (DMEM, 56–439) was obtained from Hazelton Research Products, Denver, PA; L-glutamine, penicillin/streptomycin (10,000 U penicillin/mL and 10 mg streptomycin/mL), and fetal bovine serum were obtained from Whittaker Bioproducts, Walkersville, MD; defined bovine calf serum was obtained from Hyclone Laboratories, Logan UT. Trypsin-EDTA (10x, 0.5% trypsin, 5.3 mM EDTA) was obtained from Gibco Laboratories, Grand Island, NY. m-AMSA was obtained from the Drug Synthesis and Chemistry Branch of the Developmental Therapeutics Program at the National Cancer Institute. The radiolabeled compounds [^{3}H]thymidine (75 Ci/mmol) and [α-^{32}P]dCTP (3000 Ci/mmol) were obtained from ICN Radiochemicals, Irvine, CA, and DuPont NEN Research Products, Boston, MA, respectively. Nuclease S_1 was obtained from Pharmacia LKB Biotechnology, Inc., Piscataway, NJ; DMSO, proteinase K, and RNase A were obtained from the Sigma Chemical Co., St. Louis, MO. The c-*myc* probe, an *Eco*RI/*Cla*I fragment of pMC41 3RC containing the third exon of the human c-*myc* gene [17], was provided by Dr. Eric Westin of the Medical College of Virginia. The restriction endonucleases *Eco*RI and *Hin*dIII were obtained from New England Biolabs, Beverley, MA, and the nick translation kit was obtained from GIBCO BRL, Gaithersburg, MD.

Cell culture and growth inhibition. The human breast tumor cell line MCF-7 (obtained from Dr. Ken Cowan, National Cancer Institute) was grown in DMEM supplemented with glutamine (0.292 mg/mL), penicillin/streptomycin (0.5 mL/100 mL medium), 5% fetal bovine serum, and 5% defined bovine serum at 37°, under 5% CO_2. Drug effects on cell proliferation were determined as described previously [18]. In the present studies, cells were incubated for 2 hr in the presence of m-AMSA before analysis of viable cell number using the MTT tetrazolium dye assay [19].

DNA cleavage in intact cells. Bulk (single-strand) damage to DNA was determined using the alkaline unwinding procedure of Kanter and Schwartz [20], as described in detail previously [6]. DNA cleavage was monitored based on the differential binding of a Hoechst dye to single-stranded (ssDNA) and double-stranded (dsDNA) DNA. Briefly, cells in 75 cm^2 T flasks (Costar) were incubated with m-AMSA or the vehicle control (DMSO) for 2 hr, washed with phosphate-buffered saline (PBS, pH 7.4). released from flasks by incubation with 0.05 mg/mL trypsin in 0.02 mg/mL EDTA for 5 min at 37°, and collected in ice-cold PBS. Each condition (6×10^6 cells/condition) was subdivided into three different groups: (1) dsDNA control, with no alkali-induced DNA unwinding, (2) cells treated for a 10-min alkaline unwinding period, and (3) total ssDNA, where cells were sonicated before alkaline unwinding. F values, defined as F = (alkali-treated DNA − ssDNA)/(dsDNA control − ssDNA), were determined in quadruplicate, and then converted to rad equivalents based on standardization of DNA damage using a ^{137}Cs irradiator to produce graded amounts of strand breakage.

Induction of DNA strand breaks by alkaline and neutral elution. Strand breaks in DNA were analyzed further using either alkaline elution for single-strand breaks [21] or the neutral elution assay procedure for double-strand breaks [21], as described in detail previously [18, 22]. Cells were labeled for 24 hr with 0.1 μCi/nmol [^{3}H]thymidine followed by washing and incubation for an additional 24 hr in thymidine-free medium prior to incubation with drug and processing as described for the alkaline unwinding assay. Approximately 5×10^5 cells were lysed on either polyvinyl chloride filters (Gelman Corp., Ann Arbor, MI) for alkaline elution or polycarbonate filters (Nucleopore Corp., Cambridge, MA) with SDS (2%)/EDTA (0.02%) for neutral elution. Proteinase K (2 mg/mL) was used to eliminate DNA–protein cross-linking and to distinguish between direct and protein-associated strand breaks in the alkaline elution assay. DNA was eluted using tetrapropylammonium hydroxide at either pH 12.1 (for alkaline elution) or pH 9.6 to 10 (for neutral elution) at a flow rate of 0.8 mL/hr; fractions were collected over a 17-hr period, and analyzed by scintillation counting. Damage was normalized based on radiation equivalence determined by exposure of MCF-7 cells to various doses of ionizing radiation using a ^{137}C source.

Combined alkaline unwinding/Southern blotting assay. The combined alkaline unwinding/Southern blotting (AU/SB) assay was performed as previously described [23]. Briefly, MCF-7 cells in log-phase growth were labeled with [^{3}H]thymidine (0.1 μCi/mL) for 24 hr, followed by a chase with unlabeled medium for approximately 16 hr. Cells ($10–25 \times 10^6$/condition) were removed from the tissue culture dishes with trypsin-EDTA, resuspended in approximately 10 mL of medium, and allowed to equilibrate for 1 hr at 37°. Cells were then treated with various concentrations of m-AMSA, or the vehicle control DMSO, for 1 hr. Following treatment, cells were centrifuged at 500 *g* at 0°, resuspended in cold PBS, and placed on ice. For DNA damage reversal studies, cells were resuspended in warm medium and incubated under cell culture conditions for various periods of time. Cells were then immediately placed on ice and centrifuged at 500 *g*, and resuspended in cold PBS. Alkali-induced unwinding of the DNA was initiated with the addition of 2 mL of unwinding solution (0.044 M NaOH, 1.125 M NaCl, at 22°). Unwinding was terminated with the addition of 2 mL acetic acid (0.054 M). (For control groups with no unwinding, the unwinding solution and the neutralization solution were added simultaneously.) Subsequently, unwound

single-stranded DNA was digested with nuclease S_1, and proteins were degraded with proteinase K.

The overall per cent of double-stranded DNA (%dsDNA) remaining after the unwinding was calculated by determining the relative amounts of DNA in trichloroacetic acid (TCA)-soluble and TCA-precipitable fractions. A portion of each sample (0.1 mL) plus 0.1 mL salmon sperm DNA (100 μg/mL) were precipitated with TCA (10%) on ice for 5 min. After centrifugation (2200 *g* for 5 min), the supernatant was removed and added to 6 mL of Safety Solve scintillation fluid (RPI Corp., Mount Prospect, IL). The precipitate was dissolved in NaOH (0.1 N) for 10 min, and added to scintillation fluid. The amount of labeled DNA in each fraction was determined using a Beckman LS 1801 scintillation counter. The %dsDNA was determined as the proportion of total disintegrations per min (dpm) that were acid-precipitable. Because the kinetics of the alkali-induced DNA unwinding process imply a logarithmic relationship between the number of strand breaks and the %dsDNA [24, 25], the reversal of m-AMSA-induced damage was determined as:

[log (%dsDNA of reversed damage/%dsDNA of unreversed damage)/log (%dsDNA of untreated control/%dsDNA of unreversed damage)] × 100.

Following phenol:chloroform extraction of the DNA, and resuspension in Tris/10 mM EDTA, acid-precipitable dpm were again determined. These data, along with the pre-extraction %dsDNA, were used to calculate the amount of DNA to be digested for each sample as described in detail previously [23]. This procedure corrects for any differences in the concentration of the samples that may have occurred during the course of the purification, and ensures that the amount of acid-precipitable DNA used for electrophoresis and Southern blotting reflects the decrease in %dsDNA due to alkaline unwinding. Control levels of acid-precipitable DNA were determined by averaging values from two sham unwinding controls, one with and one without drug treatment.

Southern blot analysis was performed essentially as described by Sambrook *et al.* [26]. Briefly, DNA was digested with *Eco*RI or *Hin*dIII overnight at 37°, and electrophoresis was carried out in a 0.8% agarose gel. DNA was transferred to Nytran (Schleicher & Schuell, Keene, NH) membranes and then hybridized to specific probes, which were labeled to a specific activity of about 1–3 × 10^8 cpm/μg using [α-^{32}]dCTP and a nick-translation kit. Blots were washed to remove background radioactivity and then exposed to X-ray film in the absence of an intensifying screen to increase the accuracy of the quantitation, which was performed by densitometry on a Shimadzu scanning densitometer (CS-9000).

Gene expression. After incubation with m-AMSA for appropriate times and at stated concentrations, cells were washed twice with 10 mL of ice-cold PBS (pH 7.4), and cells were lysed in 4 M guanidine isothiocyanate and 0.5% sodium lauryl sarcosine. RNA from MCF-7 cells was separated by ultra-centrifugation through a 5.7 M cesium chioride cushion at 41,000 *g* for 20 hr at 20° [6]. RNA pellets were then washed in 95% ethanol and 70% ethanol, and resuspended in Milli Q water.

RNA (10 μg) was denatured in 0.02 M morpholino propane sulfonic acid, pH 7.0, 5 mM sodium acetate, 1 mM EDTA, 2.2 M formaldehyde and 50% formamide. The samples were separated on a 6.6% formaldehyde, 1% agarose gel [27]. Equal loading of RNA in each lane was confirmed by ethidium bromide staining. Blotting was carried out using Nytran transfer membranes (Schleicher & Schuell).

DNA and RNA biosynthesis. The effect of m-AMSA on the rate of DNA or RNA synthesis was determined by monitoring the rate of incorporation of [^{3}H]thymidine or [^{3}H]uridine into acid-precipitable material over a time course of 40 min (DNA) or 120 min (RNA), as previously described [18]. MCF-7 cells in 24-well plates (Costar) were exposed to m-

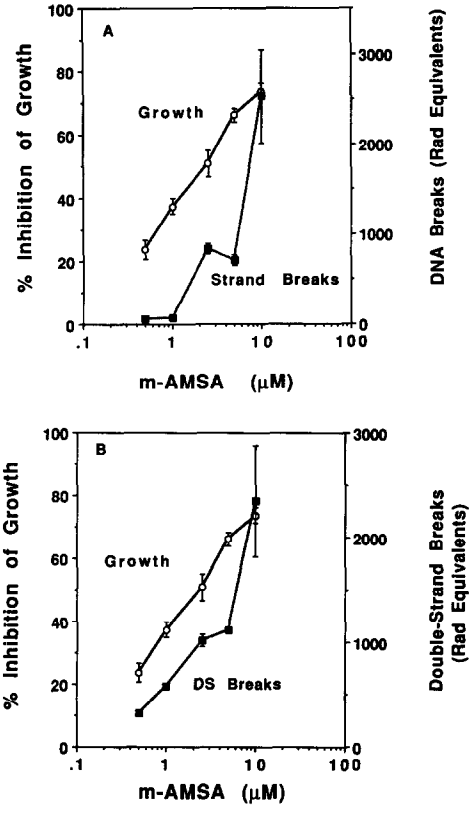

Fig. 1. Induction of strand breaks and inhibition of growth by m-AMSA in the MCF-7 breast tumor cell line. MCF-7 cells were incubated with various concentrations of m-AMSA for 2 hr. (A) Induction of DNA single-strand breaks was determined using the alkaline unwinding assay, where DNA damage were converted to rad equivalents (see Materials and Methods). Values are the means ± SEM of 6 experiments. Growth inhibition was determined using the MTT tetrazolium dye assay. Values are means ± SEM of an average of 17 determinations per drug concentration. (B) Neutral elution studies were performed to assess m-AMSA-induced double-strand breaks. DNA strand breaks were quantitated by comparison with ionizing radiation-induced damage and then converted to rad equivalents. Values are the means ± SEM of four determinations.

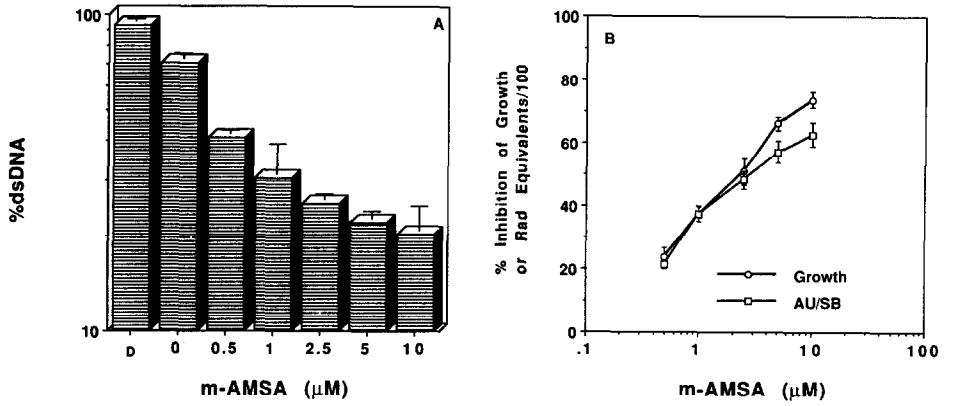

Fig. 2. Induction of strand breaks as measured by the alkaline unwinding/Southern blotting assay. MCF-7 cells were treated in suspension with various concentrations of m-AMSA for 1 hr followed by the modified alkaline unwinding method. Single-stranded DNA was specifically digested with nuclease S_1. Values in both panels A and B are means ± SEM of an average of five determinations per condition. (A) The fraction of DNA remaining double-stranded (%dsDNA) was determined by the differential solubility of the undigested dsDNA and the digested ssDNA in TCA, and graphed as a function of the concentration of m-AMSA. Column D represents a DMSO vehicle control in the absence of alkaline unwinding. Column 0 represents a DMSO control with 10 min of alkaline unwinding. (B) The average %dsDNA values determined as described in panel A were converted to rad equivalents based on ionizing radiation-induced decreases in %dsDNA, and plotted as the rad equivalents/100; error bars represent the average error, which was 6.1% of the mean. The effect of m-AMSA on growth inhibition (see Fig. 1) was also plotted for comparison.

AMSA for 2 hr and washed with Hanks' buffered salts solution (pH 7.4; Whittaker Bioproducts) at room temperature prior to analysis of [^{3}H]thymidine of [^{3}H]uridine incorporation into TCA-precipitable cpms. Per cent inhibition of DNA or RNA biosynthesis was calculated from the relative rates of incorporation of ^{3}H-labeled nucleic acid precursors in drug-treated versus untreated control cells.

RESULTS

Effects of m-AMSA on bulk damage to DNA. The influence of the aminoacridine, m-AMSA, on the integrity of cellular DNA was first examined using the alkaline unwinding assay, which provides a measure of total (single) strand breaks. Fig. 1A compares the profile of bulk DNA damage to that of growth inhibition, as measured by the MTT dye assay [19]. While bulk damage to DNA has been shown to correspond with the antiproliferative or cytotoxic effects of topoisomerase II inhibitors, such an association was not apparent in this cell line. For instance, between 0 and 5 μM m-AMSA, growth was inhibited by 66% with a concomitant induction of 700 rad equivalents of single-strand DNA cleavage. In contrast, between 5 and 10 μM m-AMSA, an insignificant change in growth inhibition (7%) was associated with induction of 1800 rad equivalents of single-strand DNA cleavage.

While m-AMSA is thought to produce primarily single-strand breaks in DNA [28], it has been suggested that double-strand breaks more closely reflect cytotoxicity [29]. Therefore, neutral elution experiments were performed to assess the relationship between m-AMSA-induced double-strand breaks and growth inhibition in the MCF-7 cell. Figure 1B compares the profile of double-strand breaks (DSBs) to growth inhibition at varied concentrations of m-AMSA. With increasing concentrations of m-AMSA, there was a corresponding increase in the rate of DNA elution, indicative of increased DNA DSBs. While there was parallelism between growth inhibition and induction of DSBs over the concentration range of 0.5 through 2.5 μM m-AMSA, this apparent correlation was lost between 2.5 and 10 μM m-AMSA. For instance, between 2.5 and 5 μM m-AMSA, growth inhibition increased from 51 to 65% with no increase in DNA damage, while between 5 and 10 μM m-AMSAS, growth inhibition increased from 65 to 74% and was accompanied by an additional 1800 rad equivalents of double-strand cleavage. Nevertheless, an association between double-strand breaks in DNA and the antiproliferative activity of m-AMSA in the MCF-7 breast tumor cell line cannot be ruled out entirely based on these data. It should be noted that, except for the interval between 0.5 and 1 μM m-AMSA, there was a close correlation between single-strand breaks assessed by alkaline unwinding and double-strand breaks assessed using neutral elution.

To confirm the nature of the DNA strand breaks induced by m-AMSA in the MCF-7 breast tumor cells, alkaline elution studies were performed in the absence and presence of proteinase K. At 10 μM m-AMSA, the breaks induced by m-AMSA in the MCF7 cell were primarily protein-associated (not shown), consistent with inhibition of topoisomerase II [30].

Assessment of chromatin region-specific DNA damage. Since it has been shown that certain DNA-damaging agents have the ability to preferentially

target specific chromatin regions [23], it was of interest to determine whether m-AMSA-induced DNA damage was also localized to specific genomic regions. m-AMSA-induced topoisomerase II cleavage sites have been mapped to the promoter region of the nuclear oncogene c-*myc* in cell lines with amplified c-*myc* [9–11, 31]. Because c-*myc* is known to be an important factor for growth in the MCF-7 tumor cell line [13–15], the susceptibility of this genomic region to m-AMSA-induced DNA damage was compared with that of other chromatin regions as well as with damage in bulk DNA.

The modified unwinding conditions of the AU/SB assay (without Southern blotting) were utilized to examine the profile of m-AMSA-induced DNA damage throughout the bulk of the genome. In this procedure, DNA is unwound in the presence of high salt concentrations (1 M) to ensure that non-covalent DNA/protein interactions do not interfere with the unwinding process. After drug treatment, unwinding of DNA in alkali, and digestion of single-stranded DNA with nuclease S_1, the relative fraction of DNA remaining double-stranded (%dsDNA) was determined by the differential solubility of intact double- and digested single-stranded DNA in TCA. Figure 2A shows that the %dsDNA decreased as a function of the concentration of m-AMSA, reflecting the induction of strand breaks that accelerate the rate of DNA unwinding in alkali. The m-AMSA-induced DNA damage began to saturate at about 2.5 μM, which is in agreement with a previous report by Zwelling *et al.* [28]. Column D in Fig. 2A shows a control where cells were treated with only the vehicle (DMSO) in the absence of unwinding; under this condition, at least 92% of the DNA remained double stranded. Furthermore, m-AMSA treatment had no significant effect on the %dsDNA in the absence of alkaline unwinding (not shown), indicating the necessity for the unwinding step in the detection of DNA strand breaks in this assay.

In an additional control, where cells were exposed to DMSO and permitted to unwind in alkali for 10 min (Fig. 2A, column 0), the %dsDNA decreased to 71%. The decrease in %dsDNA is thought to be the result of alkali-induced unwinding from endogenous strand breaks that may result from ongoing transcription and replication. Therefore, all data were normalized to correct for this control unwinding. These data were converted to radiation equivalents based on the capacity of ionizing radiation to induce DNA damage [23], and plotted as a function of the concentration of m-AMSA (Fig. 2B). It is evident that the profile of m-AMSA-induced DNA strand breakage, as measured using the alkaline/high salt conditions of the AU/SB assay, parallels the profile for inhibition of growth induced by m-AMSA in this tumor cell line. Thus, this modified alkaline unwinding method *may* provide a more accurate reflection of m-AMSA-induced damage associated with growth inhibition than do conventional assays for DNA damage.*

* Rad equivalents were determined by comparison with a standard curve generated from %dsDNA determinations in irradiated cells. However, because of an apparent plateau in unwinding at higher doses of γ-rays, there is a high degree of uncertainty in the values indicated for 5 and 10 μM m-AMSA.

To determine whether certain genomic regions may be more sensitive than bulk DNA to m-AMSA-induced DNA damage, the combined AU/SB assay was further utilized to assess DNA strand breaks induced by m-AMSA within specific large-scale regions (about 1 megabase) of the genome. The chromatin domains examined included the non-transcribed, centromeric, α-satellite repeat region specific for chromosome 17, the L1 *Hin*dIII repeat, as well as two actively transcribed regions encompassing c-*myc* and c-*fos*.

The top panel of Fig. 3 (lanes 2–8) presents an autoradiograph from an AU/SB assay where MCF-7 breast tumor cells were exposed to 0.5 and 10 μM m-AMSA and hybridized with a probe specific for c-*myc*. For a given period on unwinding (10 min for lanes 3–5), there was a concentration-dependent decrease in the hybridization signal, indicative of increasing levels of damage within the 1 megabase region encompassing the c-*myc* locus. This was also evident in lanes 6–8, which were identical to lanes 3–5 except that an unwinding time of 30 min was utilized. Also, for a given concentration and increasing unwinding times (lanes 3–5 compared with lanes 6–8) there was a time-dependent decrease in the hybridization signal, indicative of the time dependency of alkali-induced DNA unwinding.

When this assay was performed in the absence of alkaline unwinding (i.e. essentially standard Southern blotting), 10 μM m-AMSA, which inhibits growth of MCF-7 breast tumor cells by 73%, produced a 15% decrease in the hybridization intensity of c-*myc* (compare lane 1, no drug, with lane 2, 10 μM m-AMSA). However, this decrease was not specific for the c-*myc* region, as a similar decrease was observed in the α-satellite region (data not shown). At 1 μM m-AMSA, there was no detectable decrease in the hybridization intensity of either the c-*myc* or the α-satellite (data not shown).

After these blots were stripped and rehybridized with radiolabeled probes specific for α-satellite, L1, and c-*fos*, hybridization signals were quantitated, normalized to control for baseline unwinding (sham drug treatment with alkaline unwinding, see Fig. 2A, 0 column), and plotted as the fraction of hybridization sequence remaining double stranded (F_{DS}) versus the concentration of m-AMSA (Fig. 3, bottom panel).

At an m-AMSA concentration of 0.5 μM, the regions encompassing c-*fos* and the L1 repeat appeared to be preferentially sensitive when compared with the bulk of the genome or with α-satellite DNA. However, at this concentration the c-*myc* region appeared to be only slightly more sensitive to m-AMSA-induced DNA damage than α-satellite DNA or the bulk of the genome. In contrast to the findings with 0.5 μM m-AMSA, 10 μM m-AMSA appeared to produce preferential damage in the regions encompassing both c-*myc* and c-*fos*, as well as in the L1 repeat, when compared with either α-satellite DNA or the bulk of the genome. DNA damage analysis performed at intermediate concentrations (1 and 5 μM m-AMSA) also indicated that m-AMSA-induced cleavage occurred preferentially within the c-*myc*, c-*fos*, and L1 repeat chromatin regions when compared with

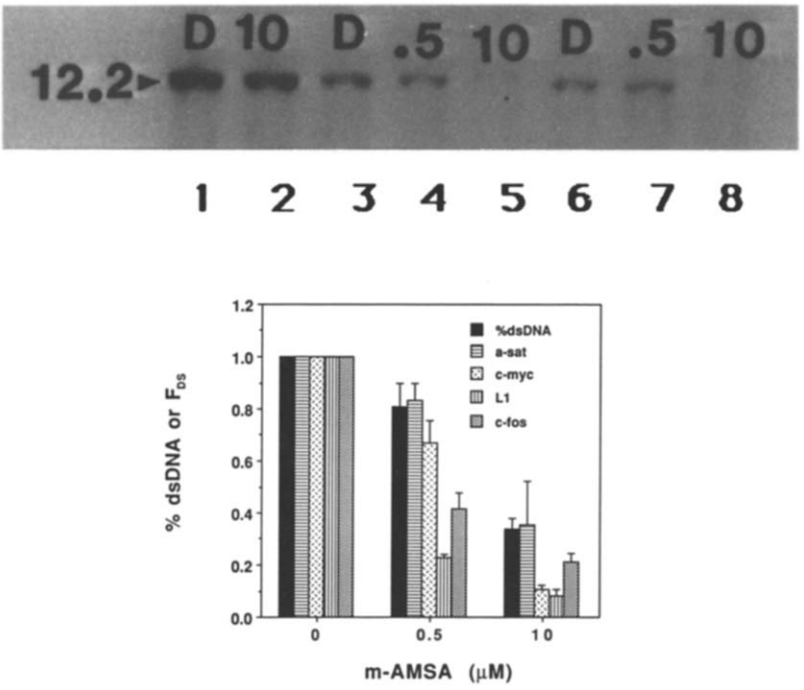

Fig. 3. Alkaline unwinding/Southern blot analysis of m-AMSA-induced damage within regions surrounding the c-*myc* oncogene. The AU/SB assay was performed as described (see Materials and Methods). DNA was digested with *Hin*dIII, electrophoresed in a 0.7% agarose gel, followed by Southern blot analysis, where membranes were hybridized to a nick-translated c-*myc* probe. (Top panel) Lanes 1 and 2 (marked D and 10, respectively) represent standard Southern blotting (absence of alkaline unwinding, with DMSO vehicle control, and 10 μM m-AMSA, respectively. Lanes 3–5 (denoted as D, 0.5, and 10, respectively) represent the vehicle control, 0.5 μM, and 10 μM m-AMSA, respectively, with 10 min of alkaline unwinding. Lanes 6–8 represent conditions identical to those of lanes 3–5 but with an unwinding time of 30 min. (Bottom panel) Quantitative representation of damage within specific chromatin regions in MCF-7 breast tumor cells treated with m-AMSA using the AU/SB assay. Membranes were sequentially hybridized to probes specific for c-*myc*, c-*fos*, L1, and α-satellite DNA. Densitometry was performed on all autoradiographs; data were normalized to the sham drug treatment controls, and plotted as the F_{ds} (fraction of hybridization sequence remaining double-stranded after alkaline unwinding) versus the concentration of m-AMSA. Values are means ± range of at least duplicate determinations. For bulk DNA damage, which is included for comparison, the data are plotted as the %dsDNA versus the concentration of drug.

α-satellite or bulk DNA (data not shown). Overall, m-AMSA treatment resulted in a non-random distribution of DNA damage at the level of large-scale chromatin domains. Thus, this profile of m-AMSA-induced DNA damage indicates that there is heterogeneity in the susceptibility of discrete chromatin regions.

Reversal of m-AMSA-induced DNA strand breaks. It is known that the DNA repair capacity of the cell may influence its sensitivity to DNA damaging agents [32, 33]. This may be a consequence of intragenomic repair heterogeneity, which has been shown to exist for UV-induced DNA damage within the c-*myc* locus [34]. Therefore, the AU/SB assay was utilized to examine the reversal of m-AMSA-induced DNA strand breaks in the bulk of the genome as well as within specific chromatin regions. It is important to note that the m-AMSA-induced DNA–topoisomerase II cleavable complex is thought to be readily reversible [28].

Using a sub-maximal growth inhibitory concentration of m-AMSA (5 μM, where growth is inhibited by 65%) reversal of DNA damage was measured by incubating drug-treated MCF-7 cells in warm (37°) medium in the absence of drug for various time periods up to 3 hr. Determination of bulk DNA damage after cells were incubated in drug-free medium (Fig. 4a) indicated an initial rapid reversal of about 40% of the m-AMSA (5 μM) induced strand breaks followed by an extended period with little additional reversal of DNA strand breaks (see Materials and Methods for a definition of per cent reversal). The maximum extent of reversal after 2–3 hr of incubation in drug-free medium was about 60%, indicating that at least 40% of the total breaks were not reversed or repaired at this drug concentration (data not shown).

These results were verified using conventional alkaline unwinding methods [20]. Figure 4B represents the concentration dependency for reversal of m-AMSA-induced DNA damage. At 0.5 μM m-AMSA, there was a rapid and seemingly complete

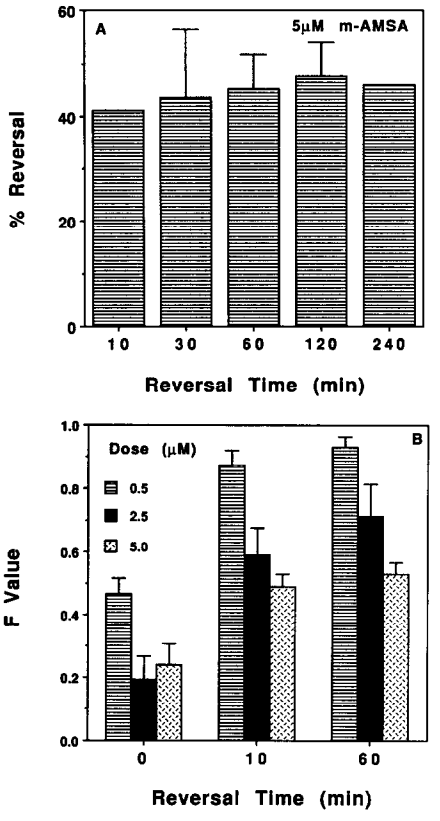

Fig. 4. Reversal of m-AMSA-induced DNA strand breaks in the bulk of the genome. After m-AMSA treatment, cells were incubated in drug-free medium at 37° for various time periods to allow for reversal of DNA damage. (A) Measurement of DNA damage reversal utilizing the modified AU/SB method. DNA damage reversal was measured as [log(%dsDNA of reversed damage/%dsDNA of unreversed damage)/log (%dsDNA of untreated control/%dsDNA of unreversed damage)] × 100. (B) DNA damage reversal as measured by the alkaline unwinding method of Kanter and Schwartz [20]. Data are plotted as the F value, which is equivalent to the %dsDNA of the AU/SB assay. Error bars represent ± SEM of four separate F value determinations.

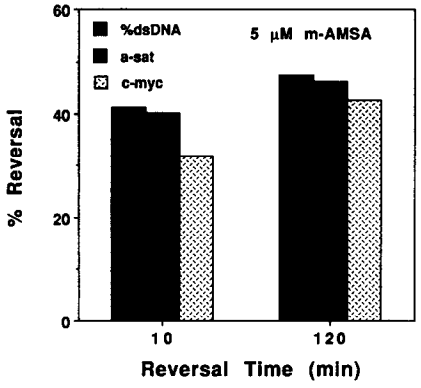

Fig. 5. Reversal of m-AMSA-induced DNA strand breaks within the regions encompassing c-*myc* and α-satellite DNA. The AU/SB assay was performed after permitting reversal of bulk damage induced by 5 μM m-AMSA. Reversal of m-AMSA-induced damage was measured and quantitated in the c-*myc* and α-satellite regions.

reversal of the damage; the F value (%dsDNA) reached 95% of vehicle control (DMSO) within 10 min of drug-free incubation, and control levels within 1 hr. In contrast, complete reversal was *not* observed with higher concentrations of m-AMSA; using 2.5 and 5 μM m-AMSA, the F values reached only 75 and 55% of control, respectively, within 1 hr. Thus, both the AU/SB assay and the standard alkaline unwinding assay indicated the presence of a subpopulation of irreversible, or at least very slowly reversing, m-AMSA-induced DNA strand breaks.

The reversal of drug-induced lesions within specific chromatin domains was also examined in the region encompassing c-*myc* and in α-satellite DNA (Fig. 5). The initial reversal (within 10 min) of breaks within the c-*myc* region appeared to be slightly less than that within the α-satellite region; however, after 1 hr the profile of reversal within specific chromatin regions appeared to reflect that occurring within the bulk of the genome.

Effects of m-AMSA on gene expression. It is possible that one consequence of the induction of lesions within the vicinity of the c-*myc* gene could be alterations in expression of this gene, particularly since Riou *et al.* [9] have reported reduced c-*myc* expression associated with m-AMSA treatment. Figure 6A presents the results of northern blotting studies to assess the effects of m-AMSA on c-*myc* expression; lanes 2–5 are DMSO-treated samples and lanes 6–9 are samples treated with m-AMSA. Initially, there was a marked enhancement of c-*myc* expression produced both by m-AMSA (lane 6) and by the DMSO vehicle (lane 2); however, after 3 hr, c-*myc* expression in m-AMSA-treated cells declined to 9% of DMSO controls (compare lanes 4 and 8). Glyceraldehyde phosphate dehydrogenase (GAPD) and β-actin RNA levels, which were utilized as controls, showed slight perturbations, but essentially remained at control levels after 3 hr of m-AMSA treatment (panels C and B in Fig. 6). Both drug and vehicle generally induced transient increases in expression of the early response gene, c-*fos*; after 3 hr of drug treatment, steady-state c-*fos* mRNA levels were restored to baseline values (data not shown).

The concentration-dependent reduction in c-*myc* expression was monitored at 3 hr, a time point where the decrease in steady-state c-*myc* levels appeared to plateau. The c-*myc* mRNA levels (panel A in Fig. 7), as determined by densitometry or Betascope analysis, were compared with those for β-actin (panel B in Fig. 7). The c-*myc*/β-actin ratio decreased in a concentration-dependent manner from 0.69 at 0.5 μM m-AMSA to 0.03 at 10 μM m-AMSA. A similar relationship was observed when c-*myc* levels were compared to GAPD; the c-*myc*/GAPD ratio was 0.64 at 0.5 μM m-AMSA and 0.04 at 10 μM m-

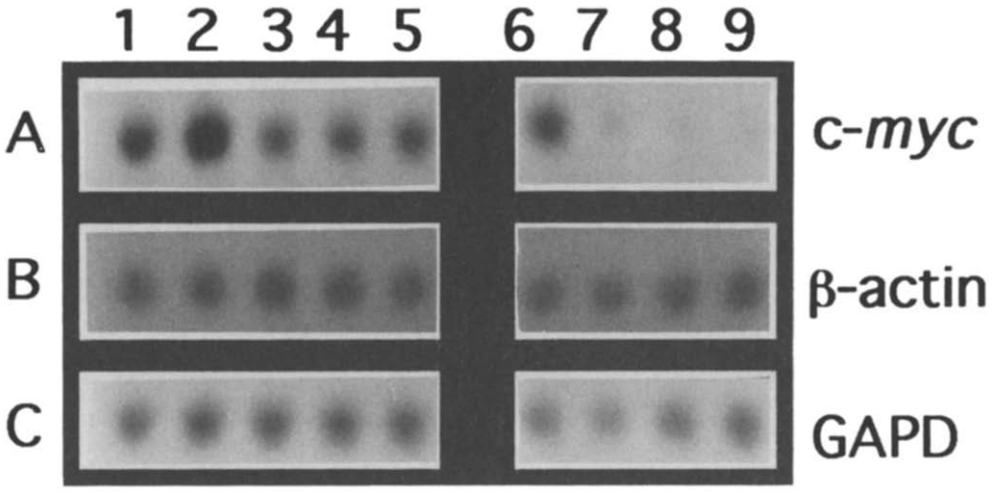

Fig. 6. Northern blot of c-*myc*, β-actin, and GAPD expression in MCF-7 cells after m-AMSA treatment for various times. Cells were exposed to either a volume equivalent of DMSO, (the vehicle control), or 10 μM m-AMSA, for 1 hr (lanes 2 and 6, respectively), 2 hr (lanes 3 and 7), 3 hr (lanes 4 and 8), or 4 hr (lanes 5 and 9). Lane 1 represents a sham drug treatment control processed at the beginning of the experiment to examine normal steady-state mRNA levels.

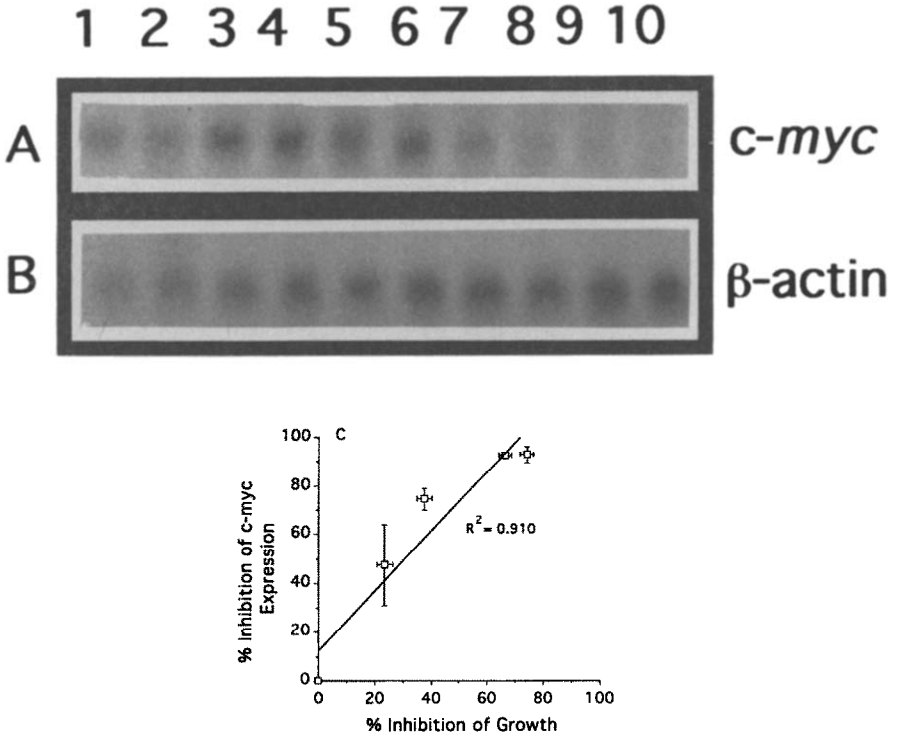

Fig. 7. Northern blot of c-*myc* and β-actin expression in MCF-7 cells after treatment with various concentrations of m-AMSA. Cells were treated for 3 hr with 0.5, 1.0, 5.0, and 10 μM m-AMSA (lanes 7–10). For controls, cells were treated with volume equivalents of DMSO at each concentration (lanes 3–6). Lanes 1 and 2 represent sham drug treatment control samples taken at 0 and 3 hr after the beginning of the experiment to examine normal steady-state fluctuations. RNA was extracted, and northern blots were then probed for c-*myc* mRNA (A), or β-actin mRNA (B). (C) Relationship between concentration-dependent inhibition of c-*myc* expression in MCF-7 cells exposed to varied concentrations of mAMSA and the corresponding alterations in growth for two experiments.

AMSA (data not shown). Thus, m-AMSA treatment appears to produce a specific decrease in c-*myc* expression, but not in the expression of the "housekeeping genes" β-actin or GAPD.

To determine whether a relationship exists between the capacity of m-AMSA to reduce c-*myc* expression and its effects on growth of the MCF-7 cells, the effects of m-AMSA on c-*myc* expression were compared with its effects on cell growth. In Fig. 7C, the per cent inhibition of c-*myc* expression, from several experiments, expressed as [1-c-*myc*/β-actin)] × 100, is graphed as a function of the inhibition of cell proliferation. Although the absolute magnitude of inhibition of the two events differed at any given concentration of m-AMSA, there appeared to be a consistent relationship between the antiproliferative effects of m-AMSA and reduction of c-*myc* expression.

Effect of m-AMSA on macromolecular biosynthesis. In view of the fact that c-*myc* expression has been correlated closely with cellular proliferation [14–16], and that MYC protein is associated with the nuclear matrix, specifically during S phase [12], the capacity of the aminoacridine, m-AMSA, to inhibit DNA synthesis was evaluated by monitoring the incorporation of radiolabeled precursors into acid-precipitable material. The concentration-dependent effects of m-AMSA on DNA biosynthesis, which were measured immediately after a 2-hr exposure to drug, closely paralleled the inhibition of cell growth by m-AMSA assessed 72 hr after exposure to drug (not shown). This observation suggests that inhibition of DNA synthesis may be an early effect on cellular function, which could lead to inhibition of cell growth.

The effect of m-AMSA on DNA biosynthesis was not accompanied by a parallel effect on RNA synthesis; 10 μM m-AMSA, the highest concentration used in the growth studies, reduced bulk RNA synthesis by only about 30–40%, an effect that was sustained over 2 hr (data not shown). This modest effect of RNA biosynthesis appeared to be an effect of the DMSO vehicle used to dissolve the drug, as similar decreases were also observed in vehicle controls. Thus, unlike other intercalating topoisomerase II inhibitors such as Adriamycin® and daunorubicin [18, 35], m-AMSA appeared to have little appreciable effect on RNA synthesis.

DISCUSSION

Induction of DNA damage by m-AMSA. Topoisomerase II inhibitors, such as m-AMSA, are thought to express their cytostatic and cytotoxic effects by interfering with the capacity of topoisomerase II to religate DNA, resulting in the induction of protein-associated strand breaks DNA [1–3]. This concept is based, in part, on correlations observed between growth inhibition/cell killing and the induction of DNA strand breakage [5]. However, previous studies in our laboratories utilizing the H-35 rat hepatoma cell model [6] and the MCF-7 breast tumor cell line [16], as well as work by other investigators [36], demonstrated an apparent dissociation between bulk damage to DNA and the antiproliferative activities of topoisomerase II inhibitors. The lack of a correlation observed in some cell lines does not rule out the possibility that breaks in DNA are responsible for drug toxicity in other tumor cell models. In any event, it appears that much of the damage in DNA detected by conventional assays may occur at sites in DNA that are not critical to the maintenance of normal cellular function. It is for this reason that the AU/SB assay was developed [23], to assess damage to specific genomic regions that may influence cell growth.

In the present studies, DNA damage produced by m-AMSA and measured using either the alkaline unwinding assay (for single-strand breaks) or the neutral elution procedure (for double-strand breaks) failed to show a consistent relationship with growth inhibition. In contrast, an excellent correlation was observed between antiproliferative activity and DNA damage measured when alkaline unwinding was performed utilizing the high salt conditions of the alkaline unwinding/Southern blotting procedure; this may be related to the fact that proteins which are non-covalently bound to the DNA, and which may interfere with unwinding, are removed [37]. Removal of these proteins would also result in disruption of the nuclear matrix; because topoisomerase II has been localized to the matrix [38, 39], it follows that m-AMSA-induced breaks may also be localized there. Indeed, m-AMSA-induced cleavage sites have been shown to preferentially occur within nuclear matrix-associated DNA [40]. Thus, the modified alkaline unwinding assay may detect the effects of DNA-damaging agents that target nuclear-matrix associated DNA more proficiently than conventional assays for DNA damage.

Standard Southern blotting was employed to detect m-AMSA-induced damage at the level of the gene. However, in contrast to the work of Riou *et al.* and Pommier *et al.* [10, 11, 31] who detected damage within c-*myc* using NCI-N417, a small cell lung carcinoma cell line, no cleavage sites were detectable within the c-*myc* gene at m-AMSA concentrations up to 10 μM. This difference in cleavage detection is most likely due to the fact that the c-*myc* gene is amplified to about 40–50 copies in the NCI-N417 cell line. Thus, gene amplification can apparently permit detection of breaks even in the absence of DNA unwinding.

In contrast to direct Southern blotting, the AU/SB assay permits the detection of damage within large-scale unamplified genomic regions and permits comparison of the susceptibility of a number of chromatin regions to m-AMSA-induced DNA damage. One factor that may account for this increase in sensitivity is the size of the region, or target, being examined. It is estimated from previous studies [23] that the AU/SB assay, depending on the alkaline unwinding time, detects damage within regions upwards of 1 megabase in size. Exposure to 10 μM m-AMSA produced about 6200 rad equivalents of DNA damage (see Fig. 2B). Based on studies by Kohn *et al.* [21], this represents a DNA strand break about every 200,000 base pairs. Thus, the target size of the AU/SB assay is about 5-fold greater than the density of breaks, and this amount of DNA strand breaks should be easily detectable

using the AU/SB assay. Based on the size of restriction fragments for c-*myc* and α-satellite produced for conventional Southern blotting, which are about 13 and 1.4 kb, respectively, the target size is at least about 15-fold smaller than the average density of m-AMSA-induced DNA strand breaks. Thus, even 10 μM m-AMSA, which produces a strand break about every 2×10^5 bases, would not be expected to induce enough DNA damage within these regions to be detectable with standard Southern blotting, unless these regions were at least 20-fold more susceptible to DNA damage than the bulk of the genome.

Another factor that may enhance the sensitivity of the AU/SB assay is its capacity to detect DSB, SSB, and alkali-labile lesions. As opposed to direct Southern blotting, which requires a DSB within the restriction fragment being probed to produce a decrease in the hybridization intensity, alkaline-induced DNA unwinding proceeds from SSB, DSB, as well as alkali-labile lesions (this last type of lesion is probably more important for non-topoisomerase II-induced damage; see Ref. 23).

Region-specific differences in the susceptibility to m-AMSA-induced DNA damage were detected in the present studies. At a relatively low dose of 0.5 μM m-AMSA, the L1 and c-*fos* regions appeared to be more sensitive than bulk DNA, α-satellite DNA, or the c-*myc* region. At 10 μM m-AMSA, the c-*myc* region as well as c-*fos* and L1 appeared to be hypersensitive to DNA damage when compared with the bulk of the genome, or the α-satellite region. It is unlikely that the relative insensitivity of the α-satellite region to topoisomerase II-induced DNA damage is an experimental artifact related to its high copy number since the highly repetitive L1 exhibited a different pattern of susceptibility. Based on theoretical considerations [23], the gene copy number would not be expected to influence the results derived from the AU/SB assay. The sensitivity of the c-*fos* and c-*myc* regions at higher concentrations of m-AMSA may, in part, reflect the fact that transcribed regions have a more open chromatin structure as measured by DNase I hypersensitivity [41]. In fact, c-*myc* has been shown to contain m-AMSA-stimulated topoisomerase II cleavage sites that grossly overlap with DNase I hypertensive sites [49]. This, however, does not explain the relative insensitivity of the c-*myc* region at lower m-AMSA concentrations.

It is unlikely that transcriptional activity alone fully determines the susceptibility of a region to DNA damage by a drug such as m-AMSA, since topoisomerase II cleavage sites are known to be associated with both transcriptionally active and inactive regions [42]. The susceptibility of the L1, interspersed repeat sequence to m-AMSA-induced damage, which more closely resembled that of the actively transcribed regions than the inactive α-satellite region, highlights this point. This repeated sequence localizes to the Giemsa dark staining regions of chromosomes; thus, L1 is not thought to reflect actively transcribed genomic regions but is associated with tissue-specific genes, most of which will not be actively transcribed [43, 44], although L1-containing transcripts can be detected (unpublished results and ref 45). This repetitive element is unlike α-satellite repetitive elements in that it is not repeated tandemly but interspersed throughout the genome. It has been identified within several introns [46, 47], and between genes [48]. Our results thus suggest that there may be little difference between chromatin corresponding to G-light bands (such as c-*fos* and c-*myc*) and G-dark bands (tissue specific genes, as represented by L1) in the susceptibility to drug-stimulated topoisomerase II-mediated damage. Region-specific DNA damage has also been observed for VM-26, where both the actively transcribed c-*myc* region and the inactive β-globin region were more susceptible than both the bulk of the genome and the α-satellite region [16]. Thus, the *potential* for transcription may necessitate chromosomal structures or elements (i.e. topoisomerase II cleavage sites; see below) that are particularly susceptible to m-AMSA-induced, topoisomerase II-mediated DNA damage.

These studies indicate that m-AMSA induces DNA damage with great heterogeneity at the larger scale chromatin level. Consequently, m-AMSA, as well as other topoisomerase II inhibitors, exhibit DNA damage selectivity at the DNA sequence level [49] and at several higher levels of chromatin organization (results presented here and Refs. 10, 11, 31 and 40). However, the relationship between this region-specific DNA damage and growth inhibition remains to be determined.

Reversal of m-AMSA-induced DNA damage. It has been shown that m-AMSA-induced DNA strand breaks are rapidly reversed as measured by either alkaline elution [28] or alkaline unwinding [50]. The incomplete reversal of DNA strand breaks noted here (i.e. 40% residual damage) occurred at relatively high concentrations of m-AMSA. Incomplete or slowed reversal of DNA damage has also been observed previously at high m-AMSA concentrations by other investigators [28, 51]. Recently, a topoisomerase II inhibitor-induced incomplete reversion complex was studied at the molecular level [52], where it was shown to encompass a DNA–protein cross-link as well as a single-strand break. It is possible that the irreversible or at least slowly reversible m-AMSA-induced DNA strand breaks, either within the bulk of the genome or within critical genomic regions, such as c-*myc*, may contribute to the antitumor activity of m-AMSA at elevated drug concentrations.

The kinetic profile of the reversal of damage within c-*myc* appears to parallel the reversal of damage throughout the genome. In contrast to reports in another system [34], the regions surrounding c-*myc* failed to demonstrate enhanced damage reversal. In fact, there appeared to be a slight, but reproducible lag in the repair kinetics within the c-*myc* locus (see Fig. 5b) at 10 min which disappeared with longer repair times.

Effects of m-AMSA on c-myc *expression.* The capacity of m-AMSA to produce concentration-dependent reductions in both c-*myc* expression and DNA synthesis, which closely parallel and precede growth inhibition in the MCF-7 cell line, suggests that changes in c-*myc* expression may represent an early response to topoisomerase II-mediated damage.

It appears possible that, in response to DNA damage, either throughout the genome or within specific regions, there is a reduction in c-*myc* expression, which leads to a corresponding inhibition of DNA synthesis and compromised cell growth. The decrease in c-*myc* expression is not due to a more generalized decrease in RNA synthesis; m-AMSA did not appreciably reduce either [^{3}H]uridine uptake or the levels of expression of c-*fos*, GAPD, and β-actin.

This decrease in c-*myc* expression could be the direct result of m-AMSA-induced DNA damage occurring within that region, since cleavable complex formation could represent a physical barrier to transcription. Alternatively, since strand breaks alter the topological confirmation of DNA, it is possible that the loss of torsional strain of a region would adversely affect transcription in that region [35, 53, 54].

As shown here, a possible consequence of these alterations in c-*myc* expression is inhibition of cellular proliferation. Given the proposed role of c-*myc* in replication, it is not surprising that the ability of m-AMSA to inhibit both c-*myc* expression, as well as DNA biosynthesis, is closely correlated with m-AMSA-induced inhibition of cell growth. This may be related to the capacity of m-AMSA to inhibit replicon initiation, an effect which has been shown to occur within 30 min of drug treatment [55].

Berger *et al.* [56] previously proposed that drugs such as VP-16, a topoisomerase II inhibitor, can cause deletions within essential genes, resulting in the depletion of the gene product and ultimately leading to cell death. We reported recently that VM-26, a VP-16 analog, in addition to inducing region-specific damage in MCF-7 breast tumor cells, produces a concentration-dependent decrease in c-*myc* expression which quantitatively parallels both VM-26-induced inhibition of DNA biosynthesis and cellular proliferation. Several other antitumor agents, including tumor necrosis factor, topoisomerase II poisons, alkylators, and antimetabollites, have been shown to decrease c-*myc* expression associated with compromised cellular growth [57–63].

In summary, m-AMSA-induced DNA damage occurred with great heterogeneity throughout the genome. Although the exact consequences of this damage are unknown, m-AMSA may compromise the function of critical genomic regions. Ultimately, it appears that alterations in c-*myc* expression may provide a generalized response pathway for a variety of different antitumor drugs, all of which ultimately lead to growth inhibition and cell death.

Acknowledgements—This work was supported by a Grant from the Thomas F. and Kate M. Jeffress Trust, a Grant-In-Aid to faculty at the Medical College of Virginia, a grant from the AD Williams Foundation, and NIH Grant CA-40615.

REFERENCES

1. Tewey KM, Rowe TC, Yang L, Halligan BD and Liu LF, Adriamycin-induced DNA damage mediated by mammalian DNA topoisomerase II. *Science* **226**: 466–488, 1984.
2. Tewey KM, Chen GL, Nelson EM and Lui LF, Intercalative antitumor drugs interfere with the breakage–reunion reaction of mammalian DNA topoisomerase II. *J Biol Chem* **259**: 9182–9187, 1984.
3. Chen GL, Yang L, Rowe TC, Halligan BD, Tewey KM and Lui LF, Nonintercalative antitumor drugs interfere with the breakage–reunion reaction of mammalian DNA topoisomerase II. *J Biol Chem* **259**: 13560–13566, 1984.
4. Osheroff N, Effect of antineoplastic agents on the DNA cleavage/religation reaction of eukaryotic topoisomerase II: Inhibition of DNA religion by etoposide. *Biochemistry* **28**: 6157–6160, 1989.
5. Pommier Y, Zwelling LA, Kao-Shan C-S, Wang-Peng J and Bradley MO, Correlations between intercalator-induced DNA strand breaks and sister chromatid exchanges, mutations, and cytotoxicity in Chinese hamster cells. *Cancer Res* **45**: 3143–3149, 1985.
6. Ellis AL, Munger CE, Bunch RT, Woods KE, Randolph JK, Boise L, Swerdlow PS, Zwelling LA, Hinds M, Yanovich S and Gewirtz DA, Components of intrinsic drug resistance in the rat hepatoma. *Biochem Pharmacol* **43**: 331–342, 1992.
7. Gewirtz DA, Does bulk damage to DNA explain the cytostatic and cytotoxic effects of topoisomerase II inhibitors? *Biochem Pharmacol* **42**: 2253–2258, 1991.
8. Chow K-C and Ross WE, Topoisomerase-specific drug sensitivity in relation to cell cycle progression. *Mol Cell Biol* **7**: 3119–3123, 1987.
9. Riou J-F, Lefevre D and Riou G, Stimulation of the topoisomerase II induced DNA cleavage sites in the c-*myc* protooncogene by antitumor drugs is associated with gene expression. *Biochemistry* **28**: 9104–9110, 1989.
10. Riou J-F, Vilarem M-J, Larsen JC, Multon E and Riou GF, *In vivo* and *in vitro* stimulation by antitumor drugs of the topoisomerase II-induced cleavage sites in c-*myc* protooncogene. *NCI Monogr* **4**: 41–47, 1987.
11. Pommier Y, Orr A, Kohn KW and Riou J-F, Differential effects of amsacrine and epipodophyllotoxins on topoisomerase II cleavage in human c-*myc* proto-oncogene. *Cancer Res* **52**: 3125–3130, 1992.
12. Waitz W and Loidl P, Cell cycle dependent association of c-myc protein with the nuclear matrix. *Oncogene* **6**: 29–35, 1991.
13. Watson PH, Pon RT and Shiu RP, Inhibition of c-*myc* expression by phosphorothionate antisense oligonucleotide identifies a critical role for c-*myc* in the growth of human breast cancer. *Cancer Res* **51**: 3996–4000, 1991.
14. Dubik D, Dembinski TC and Shiu RP, Stimulation of c-*myc* oncogene expression associated with estrogen-induced proliferation of human breast cancer cells. *Cancer Res* **47**: 6517–6521, 1987.
15. Dubik D and Shiu RPC, Transcription regulation of c-*myc* oncogene expression by estrogen in hormone-responsive human breast cancer cells. *J Biol Chem* **263**: 12705–12708, 1988.
16. Gewirtz DA, Orr MS, Fornari FA, Randolph JK, Yalowich JC, Ritke MK, Povirk LF and Bunch RT, Dissociation between bulk damage to DNA and the antiproliferative activity of teniposide (VM-26) in the MCF-7 breast tumor cell line: Evidence for induction of gene-specific damage and alterations in gene expression. *Cancer Res* **53**: 3547–3554, 1993.
17. Dalla Favera R, Wong-Staal F and Gallo RC, *onc* Gene amplification in promyelocytic leukemia cell HL-60 and primary leukemic cells of the same patient. *Nature* **299**: 61–63, 1982.
18. Munger C, Ellis A, Woods K, Randolph J, Yanovich S and Gewirtz D, Evidence for inhibition of growth related to compromised DNA synthesis in the interaction of daunorubicin with H-35 rat hepatoma. *Cancer Res* **48**: 2404–2411, 1988.
19. Carmichael J, DeGraff WG, Gazdar AF, Minna JD

and Mitchell JB, Evaluation of a tetrazolium-based semiautomated colorimetric assay: Assessment of chemosensitivity testing. *Cancer Res* **47**: 936–942, 1987.
20. Kanter PM and Schwartz HS, A fluorescence enhancement assay for cellular DNA damage. *Mol Pharmacol* **22**: 145–151, 1982.
21. Kohn KW, Ewig RAG, Erickson LC and Zwelling LA, Measurement of strand breaks and cross links by alkaline elution. In: *DNA Repair: A Laboratory Manual of Research Procedures* (Eds. Friedberg EC and Hanawalt PC), Vol. 1, pp. 379–401. Marcel Dekker, New York, 1981.
22. Gewirtz DA, Ellis AL, Randolph JK, Yanovich S, Swerdlow P, Povirk LF and Yalowich JC, Expression of protein-associated DNA damage in the alkaline elution assay in the absence of enzymatic deproteinization. *Cancer Commun* **1**: 175–180, 1989.
23. Bunch RT, Gewirtz DA and Povirk LF, A combined alkaline unwinding/Southern blotting assay for measuring low levels of cellular DNA breakage within specific genomic regions. *Oncol Res* **4**: 7–15, 1992.
24. Davison PF, The rate of strand separation in alkali-treated DNA. *J Mol Biol* **22**: 97–108, 1966.
25. Rydberg B, The rate of strand separation in alkali of DNA of irradiated mammalian cells. *Radiat Res* **61**: 274–287, 1975.
26. Sambrook J, Fritsch EF and Maniatis T. *Molecular Cloning: A Laboratory Manual.* Cold Spring Harbor Laboratory Press, Cold Spring Harbor, NY, 1989.
27. Thomas PS, Hybridization of denatured RNA and small DNA fragments transferred to nitrocellulose. *Proc Natl Acad Sci USA* **77**: 5201–5205, 1980.
28. Zwelling LA, Michaels S, Erickson LC, Ungerleider RS, Nichols M and Kohn KW, Protein-associated deoxyribonucleic acid strand breaks in L1210 cells treated with the deoxyribonucleic acid intercalating agents 4′-(9-acridinylamino)methanesulfon-*m*-anisidide and adriamycin. *Biochemistry* **20**: 6553–6563, 1981.
29. Obe G, Johannes C and Schulte-Frohlinde D, DNA double-strand breaks induced by sparsely ionizing radiation and endonucleases as critical lesions for cell death, chromosomal aberration, mutations and oncogenic transformation. *Mutagenesis* **7**: 3–12, 1992.
30. Nelson EM, Tewey KM and Liu LF, Mechanism of antitumor drug action: Poisoning of mammalian DNA topoisomerase II on DNA by 4′-(9-acridinylamino)-methanesulfon-*m*-anisidide. *Proc Natl Acad Sci USA* **81**: 1361–1365, 1984.
31. Riou J-F, Multon E, Vilarem M-J, Larsen C-J and Riou G, *In vivo* stimulation by antitumor drugs of the topoisomerase II induced cleavage sites in c-myc protooncogene. *Biochem Biophys Res Commun* **137**: 154–160, 1986.
32. Costa ND and Bryant PE, Repair of DNA single-strand and double strand breaks in the Chinese hamster xrs 5 mutant cell line as determined by DNA unwinding. *Mutat Res* **194**: 93–99, 1988.
33. Eguchi-Kasai K, Kosaka T, Sato K and Kaneko I, Repairability of DNA double-strand breaks and radiation sensitivity in 5 mammalian cell lines. *Int J Radiat Biol* **59**: 97–104, 1991.
34. Beecham EJ, Mushinski F, Shacter E, Potter M and Bohr VA, DNA repair in the c-*myc* proto-oncogene locus: Possible involvement in susceptibility or resistance to plasmacytoma induction in BALB/c mice. *Mol Cell Biol* **11**: 3905–3104, 1991.
35. Tarr M and van Helden PD, Inhibition of transcription by adriamycin is a consequence of the loss of negative superhelicity in DNA mediated by topoisomerase II. *Mol Cell Biochem* **93**: 141–146, 1990.
36. Chatterjee S, Divyang T, Petzold SL and Berger NA, Mechanism of epipodophyllotoxin-induced cell death in poly(adenosine diphosphate-ribose) deficient cells *Cancer Res* **50**: 2713–2718, 1990.
37. Elia MC and Bradley MO, Influence of chromatin structure on the induction of DNA double strand breaks by ionizing radiation. *Cancer Res* **52**: 1580–1586, 1992.
38. Berrios M, Osheroff N and Fischer PA, *In situ* localization of DNA topoisomerase II, a major polypeptide component of the *Drosophila* nuclear matrix fraction. *Proc Natl Acad Sci USA* **82**: 4142–4146, 1985.
39. Earnshaw WC, Halligan B, Cooke CA, Heck MMS and Lui L, Topoisomerase II is a structural component of mitotic chromosomal scaffolds. *J Cell Biol* **100**: 1706–1715, 1985.
40. Chiu S-M, Xue L-Y, Friedman LR and Oleinick NL, Comparison of DNA–protein cross-links induced by 4′-(9-acridinylamino)methanesulfon-*m*-anisidide and by γ-radiation. *Cancer Res* **49**: 910–914, 1989.
41. Villeponteau B, Lundell M and Martinson H, Torsional stress promotes the DNAase I sensitivity of active genes. *Cell* **39**: 469–478, 1984.
42. Kroeger PE and Rowe TC, Analysis of topoisomerase I and II cleavage sites on the *Drosophila* actin and Hsp70 heat shock genes. *Biochemistry* **31**: 2492–2501, 1992.
43. Manuelidis L and Ward DC, Chromosomal and nuclear distribution of the HindIII 1.9Kb human DNA repeat segment. *Chromosoma* **91**: 28–38, 1984.
44. Chen TL and Manuelidis L, SINEs and LINEs cluster in distinct DNA fragments of Giemsa band size. *Chromosoma* **98**: 309–316, 1989.
45. Skowronski J, Fanning TG and Singer MF, Unit-length line-1 transcripts in human teratocarcinoma cells. *Mol Cell Biol* **8**: 1385–1397, 1988.
46. Bottenus RE, Ichinose A and Davie EW, Nucleotide sequence of the gene for the b subunit of human factor XIII. *Biochemistry* **29**: 11195–11209, 1990.
47. Gilman JG, Brinson EC and Mishima N, The 32·6 kb Indian $\delta\beta$-thalassaemia deletion ends in a 3·kb L1 element downstream of the β-globin gene. *Br J Haematol* **82**: 417–421, 1992.
48. Tagle DA, Stanhope MJ, Siemieniak DR, Benson P, Goodman M and Slightom JL, The β-globin gene cluster of the prosimian primate *Galago crassicaudatus*: Nucleotide sequence determination of the 41-kb cluster and comparative sequence analyses. *Genomics* **13**: 741–760, 1992.
49. Pommier Y, Capranico G, Orr A and Kohn KW, Local base sequence preferences for DNA cleavage by mammalian topoisomerase II in the presence of amsacrine or teniposide. *Nucleic Acids Res* **195**: 973–980, 1991.
50. Robbie MA, Baguley BC, Denny WA, Gavin JB and Wilson WR, Mechanism of resistance of noncycling mammalian cells to 4′-(9-acridinylamino)methanesulfon-*m*-anisidide: Comparison of uptake, metabolism, and DNA breakage in log- and plateau-phase Chinese hamster fibroblast cell cultures. *Cancer Res* **48**: 310–319, 1988.
51. Bertrand R, Sarang M, Jenkin J, Kerrigan D and Pommier Y, Differential induction of secondary DNA fragmentation by topoisomerase II inhibitors in human tumor cell lines with amplified c-*myc* expression. *Cancer Res* **51**: 6280–6285, 1991.
52. Lee MP and Hsieh T-s, Incomplete reversion of double stranded DNA cleavage mediated by *Drosophila* topoisomerase II: Formation of single stranded DNA cleavage complex in the presence of an anti-tumor drug VM26. *Nucleic Acids Res* **20**: 5027–5033, 1992.
53. Rodi CP and Sauebrier W, Structure of transcriptionally active chromatin: Radiological evidence for require-

ment of torsionally constrained DNA. *J Cell Physiol* **141**: 346–352, 1989.
54. Lucknik M, Hisamutdinov TA and Georgiev GP, Inhibition of transcription of eukaryotic cells by X-irradiation: Relation to the loss of topological restraint in closed DNA loops. *Nucleic Acids Res* **16**: 5175–5189, 1988.
55. Kaufmann WK, Boyer JC, Estabrooks LL and Wilson SJ, Inhibition of replicon initiation in human cells following stabilization of topoisomerasse II–DNA cleavable complexes. *Mol Cell Biol* **11**: 3711–3718, 1991.
56. Berger NA, Chatterjee S, Schmotzer JA and Helms SR, Etoposide (VP-16-2313)-induced gene alterations: Potential contribution to cell death. *Proc Natl Acad Sci USA* **88**: 8740–8743, 1991.
57. Osanto S, Jansen R and Vloemans M, Downmodulation of c-*myc* expression by interferon α and tumor necrosis factor α precedes growth arrest in human melanoma cells. *Eur J Cancer* **28A**: 1622–1627, 1992.
58. Armstrong DR, Tan YY and Lewis M, Post-transcriptional regulation of growth related mRNA by fluorouracil, thioguanine and tamoxifen. *Proc Am Assoc Cancer Res* **27**: 19, 1986.
59. Plummer SM, Parker NJ, DeKretser TA and Wakelin LPG, Effects of intercalating antitumor drugs on c-*myc*, c-*myb* and α-acting mRNA levels and RNA synthesis in HSB2 cells. *Proc Am Assoc Cancer Res* **30**: 561, 1989.
60. Hollander MC and Fornace AJ Jr, Induction of *fos* RNA by DNA-damaging agents. *Cancer Res* **49**: 1687–1692, 1989.
61. Futscher BW and Erickson LC, Changes in c-*myc* and c-*fos* expression in a human tumor cell line following exposure to bifunctional alkylating agents. *Cancer Res* **50**: 62–66, 1990.
62. Kashani-Sabet M, Wang W and Scanlon KJ, Cyclosporin A suppresses cisplatin-induced c-*fos* gene expression in ovarian carcinoma cells. *J Biol Chem* **265**: 11285–11288, 1990.
63. Schwartz EL, Chamberlin H and Brechbuhl AB, Inhibition of c-*myc* expression in human promyelocytic leukemia and colon adenocarcinoma by 6-thioguanine. *Biochem Pharmacol* **40**: 2449–2455, 1990.